Penerbit Akademia Baru

Journal of Advanced Research in Fluid Mechanics and Thermal Sciences

Journal homepage: www.akademiabaru.com/arfmts.html
ISSN: 2289-7879

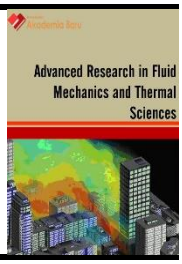

The Effect of Fluid Temperature and Crack Size toward Stress Intensity Factor on Geothermal Pipe Installations

Open Access

Khairul Anam[1,*], Anindito Purnowidodo[1], Hastono Wijaya[1]

[1] Department of Mechanical Engineering, Engineering Faculty, Brawijaya University, Malang 65145, East Java, Indonesia

ARTICLE INFO

Article history:
Received 8 October 2018
Received in revised form 21 November 2018
Accepted 2 February 2019
Available online 5 February 2019

ABSTRACT

A pipe is a fundamental component of the geothermal power plants to drain the water vapor from the inside of the earth. Structural durability is the main focus of geothermal pipe which is affected by the thermal stress caused by internal pressure and fluid temperature. In the present study, the stress intensity factor for mode I was investigated under variations of fluid temperature and crack size. A commercial finite element analysis (FEA) was used to find the highly stressed regions in the geothermal pipe by using solid-fluid interaction model and calculate the stress intensity factors. Variations used in this study are a fluid temperature in pipes of 80°C, 115°C, and 150°C and surface crack size of 1 mm, 3 mm, and 5 mm. This study used ASTM A106-B steel material which is geothermal pipe standard. The result showed that the fluid temperature and crack size in the pipe installation affects the stress intensity factor. The stress intensity factor increased with increasing the fluid temperature in the pipe and crack size. Furthermore, the pipe installation with 5mm crack size and fluid temperature in pipes 115°C and 150°C has stress intensity factor value that exceeds the fracture toughness value of the material. This condition will lead the crack to propagate along the pipe.

Keywords:
Fluid temperature, crack size, stress intensity factor, geothermal pipe

1. Introduction

Fuel from coal, natural gas, crude oil, sunlight and geothermal is needed to generate the electrical energy. Geothermal energy is an abundant energy, environmentally friendly and not dependent on weather conditions. Geothermal energy is extremely suited to meet the growing needs of electricity in the world especially Indonesia. The pipe is a component that often fails. As a result of pipe, failures can occur environmental damage, disruption to daily life, structural damage in the area around the pipe, even the emergence of the soul of the victim. Most of the pipe failures are due to the crack propagations or defects in pipe surfaces [1]. There are two possibilities due to the repair of the crack in the pipe i.e. the crack will extend slowly and penetrate the wall causing leakage before or suddenly without leakage [2].

*Corresponding author.
E-mail address: Khairul.anam27@ub.ac.id (Khairul Anam)

The pipe is a very important component for the installation of geothermal power plants to drain the water vapor from the inside of the earth. Long-term use, surface defects, or environmental conditions of geothermal pipeline installations may lead the crack to initiate. Further research is needed to predict the possibility of crack propagation in pipes.

The main objective of this present study is to investigate the cracking behavior in geothermal pipe installation by using a commercial finite element analysis (FEA). This study uses ASTM A106-B steel material which is geothermal pipe standard. FEA modelling is applied to obtain the stress distribution. The stress distribution is evaluated according to proper failure criteria to identify the highly stressed regions. The principal direction is calculated to define the crack direction. Finally, Stress intensity factors mode I (K) is calculated at these regions in the geothermal pipe during operation for various fluid temperature and surface crack size [3].

2. Methodology

A commercial FEA was used to calculate the internal pressure due to fluid velocity and temperature, the stress distributions, and the stress intensity factors for mode I. The FEA model was constructed based on ASTM A106-B steel material which is geothermal pipe standard [4]. ASTM A106-B steel is carbon steel type which is commonly used as structural materials of piping systems used in these vessels because of their lower cost and wider availability [5-8]. The outer wall diameter (D_o) of 324 mm with a thickness of 10 mm. The fluid velocity remains constant at 40 m/s [9]. The pipe act as a 90o elbow which is failure mostly occurred in this area [10-13]. Table 1 shows the numerical configurations. *T* and *a* are defined as fluid temperature and surface crack size (mm), respectively. The surface crack is considered in the present work as semi-circular crack, as shown in Figure 1.

Table 1
Numerical configurations

Temperature (°C)	Surface crack size (mm)
80	1
	3
	5
115	1
	3
	5
150	1
	3
	5

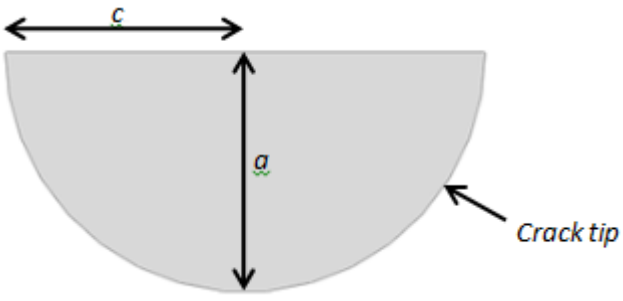

Fig. 1. Semi-circular crack type where *c* = *a*

The crack direction is defined as a principal direction of the maximum principal. The principal direction was calculated using the following equation,

$$tan\ 2\alpha = 2\tau_{xy}/(\sigma_{xx} - \sigma_{yy}) \quad (1)$$

where σ_{xx} is normal stress in x-direction, σ_{yy} is normal stress in y-direction, and τ_{xy} is shear stress [14,15]. The value of stress intensity factor calculates along the crack tip which is divided into 41 nodes.

The materials used in this study include fluid (hot steam) and pipe (ASTM A106-B steel). The material properties of fluid and pipe are shown in Table 2-5, respectively [16]. The material modeling used in this study is assumed as bilinear isotropic. And the Poisson's ratio of the geothermal pipe is also assumed constant at all temperatures.

Table 2
The material properties of fluid (hot steam)

Properties	Constant
Mass density (kg/mm^3)	5.54E-10
Dynamic viscosity (MPa.s)	1.34E-11

Table 3
The material properties of pipe (ASTM A106-B steel)

Properties	Constant
Mass density (kg/mm^3)	7.85E-06
Yield strength (MPa)	345
Ultimate tensile strength (MPa)	483
Elongation	0.35
Fracture toughness MPa√m	81

Table 4
The Young's modulus of pipe (ASTM A106-B steel) for different temperature

Young's Modulus (MPa)	Poisson's Ratio	Temperature (^{o}C)
203400	0.3	21.11
198570		93.33
198570		148.89
190900		204.44
188200		260
184000		315.56
175800		371.11

Table 5
The thermal expansion coefficient of pipe (ASTM A106-B steel) for different temperature

Coefficient of Thermal Expansion	Temperature (°C)
10.62	-17.78
11.03	37.78
11.48	93.33
11.88	148.89
12.28	204.44
12.64	260
12.82	287.78

This numerical procedure is divided into several sequences. Firstly, set up the fluid geometry and boundary conditions as shown in Figure 2. Secondly, computational fluid dynamic (CFD) was used to analyze the internal pressure by using properties of materials as listed in Table 2. Thirdly, mesh the fluid in the pipe at 25 mm by using hexagonal type. Finally, compute the internal pressure as loading in the geothermal pipe. After that, the value of internal pressure which is obtained from CFD will be used to calculate the stress distribution in the geothermal pipe by using solid-fluid interaction (SFI). Figure 3 shows the stress distribution in the pipe due to internal pressure. In Figure 3, the red area in geothermal pipe installation indicated the highly stressed regions. So, it can be determined as the position of the surface crack in the pipe. The next sequence is creating the surface crack model in the pipe which is in highly stressed regions by using structural modeling. Standard and explicit (Structural) modeling was used to calculate the stress and stress intensity factor by using properties of materials as listed in Table 3-5. Meshing along the crack used mesh control of wedge type with element number on the seed edge of 10. While around crack regions, mesh control of hexagonal type with element number on the seed edge of 30 was used.The data were collected at 41 points. An example of distance along a crack tip for 5 mm crack shown in Figure 4. Finally, the stress distribution and the stress intensity factor obtained from the simulation results.

Fig. 2. Boundary conditions and fluid flow directions

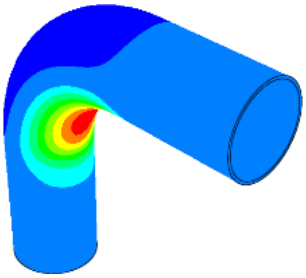

Fig. 3. The stress distribution in pipe due to internal pressure

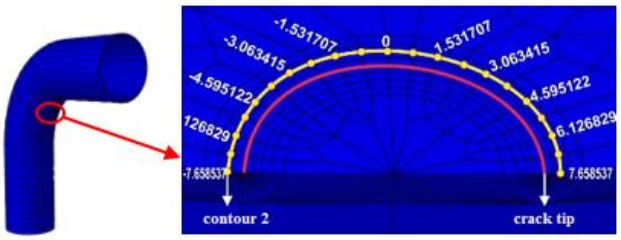

Fig. 4. The stress distribution in pipe due to internal pressure

3. Results

3.1. The Stress Intensity Factor for Mode I under Various Surface Crack Size and Fluid Temperature

The numerical results of the stress intensity factor for mode I under various surface crack size of 1 mm, 3 mm, and 5 mm (for $c = a$) at fluid temperature of 80°C, 115°C, and 150°C are shown in Figure 5–7. The order of stress intensity factor values in all temperature variations from the biggest to small is the 5mm, 3mm, and 1mm crack size. At all fluid temperature, the stress intensity factor was increased by increasing the surface crack size. Furthermore, the pipe installation with 5mm crack size and fluid temperature in pipes 115°C and 150°C has stress intensity factor value that exceeds the fracture toughness value of the material. This condition will lead the crack to propagate along the pipe. All the results have been validated by using empirical equation of stress intensity factors i.e.

$$K_I = f\sigma\sqrt{\pi a} \tag{2}$$

Where K_I is the stress intensity factor at the crack for mode 1, f is the geometry factor, σ is the working stress, and a is the crack depth [16-18]. In example the value of stress intensity factor for the surface crack size of 1 mm at temperature of 80°. The working stress of 20 MPa and the geometry factor is 0.64, so, by using Eq. (2) the value of stress intensity factors is 15.96 MPa√mm. In addition, the value of stress intensity factors from numerical result is 11.49 MPa√mm. However, both the value of stress intensity factor from empirical equation and numerical result have the same trend. It means that the numerical result is valid.

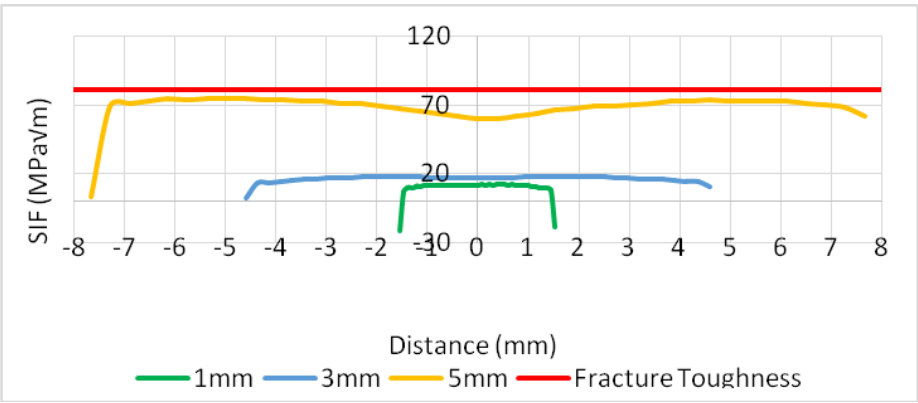

Fig. 5. Stress intensity factor for a fluid temperature of 80°C in different crack size

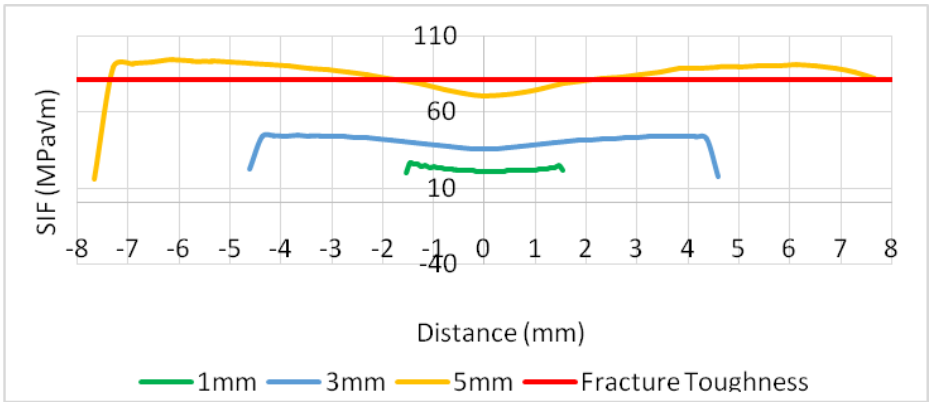

Fig. 6. Stress intensity factor for a fluid temperature of 115°C in different crack size

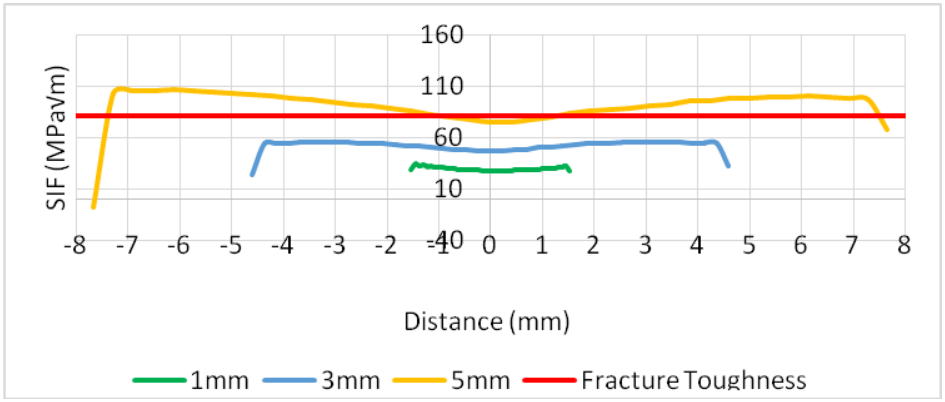

Fig. 7. Stress intensity factor for a fluid temperature of 150°C in different crack size

The numerical results of the stress intensity factor for mode I under fluid temperature of 80°C, 115°C, and 150°C at the surface crack size of 1 mm, 3 mm, and 5 mm (for $c = a$) are shown in Figure 8–10. The order of stress intensity factor values in all temperature variations from the biggest to small is the 150°C, 115°C, and 80°C. At all surface crack size, the stress intensity factor was increased by increasing the fluid temperature. Similar to previous phenomena, the pipe installation with 5mm crack size and fluid temperature in pipes 115°C and 150°C has stress intensity factor value that exceeds the fracture toughness value of the material. This condition will lead the crack to propagate along the pipe.

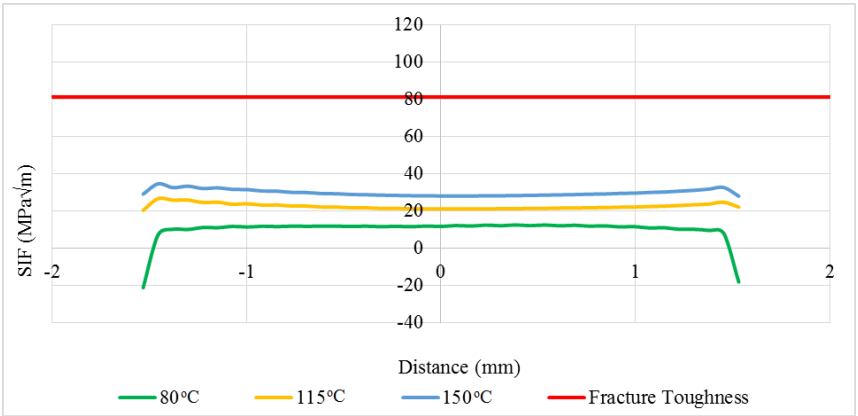

Fig. 8. Stress intensity factor for the surface crack size of 1 mm in different fluid temperature

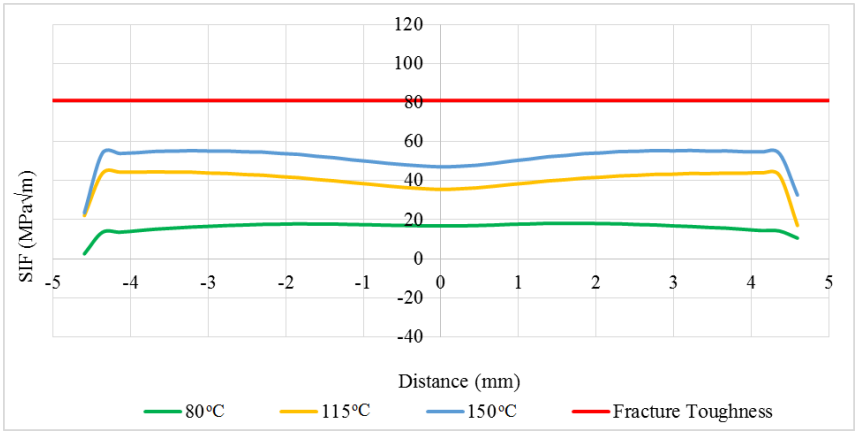

Fig. 9. Stress intensity factor for the surface crack size of 3 mm in different fluid temperature

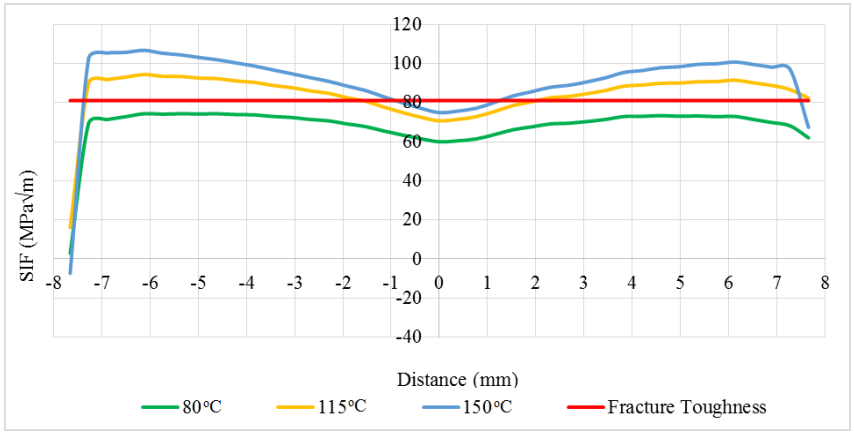

Fig. 10. Stress intensity factor for the surface crack size of 5 mm in different fluid temperature

3.2. Stress and Strain Distributions

The tendency of the stress intensity factor in all variations is the same i.e. having a large stress intensity factor at the crack tip then decreasing to the point at distance equal to zero. This phenomenon occurred due to the difference applied stress along the crack ass shown in Figure 11. The stress intensity factor increased by increasing the applied stress. In general, for all variations at the same temperature variation, the stress intensity factor increased by increasing the surface crack size which is affected by the value of the strain along the crack line itself. The larger the surface crack size means the longer the crack then the greater the strain value. So, the stress intensity factor is getting bigger either. Figure 11 also shows the strain value along the crack front which is has a similar trend with stress and stress intensity factor.

The principal stress distribution along the crack tip also affects stress intensity factor for mode I. An example of the stress distribution along the crack tip is shown in Figure 12. While the contours of stress distribution in front of the crack tip for all variations can be seen in Figure 13 (a-i). Figure 13 (a-i) shows that the area to the left of the crack tip shows the blue contours indicating that the area has a low principal stress. The closer to the crack edge of the contour color changes into the green. This indicates that the stress increases. While getting closer to the tip of the crack the color of the contour turns yellow to red. The red color indicates the location of the largest stress on the crack.

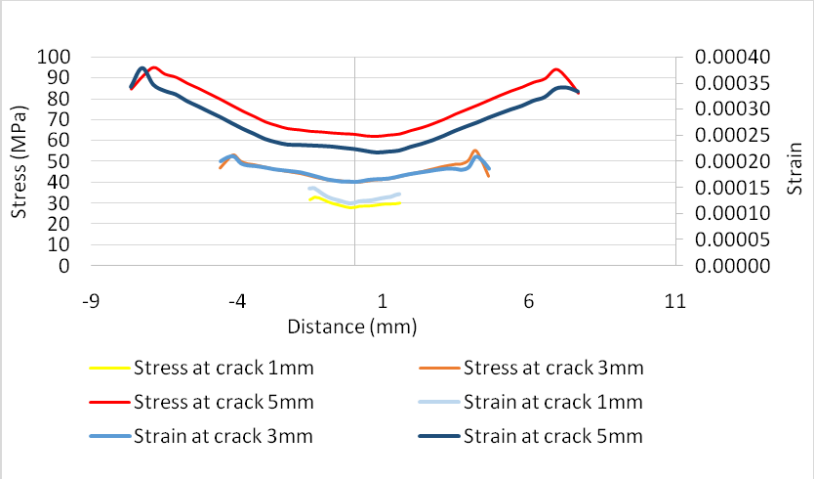

Fig. 11. Stress and strain along the crack tip in different surface crack size

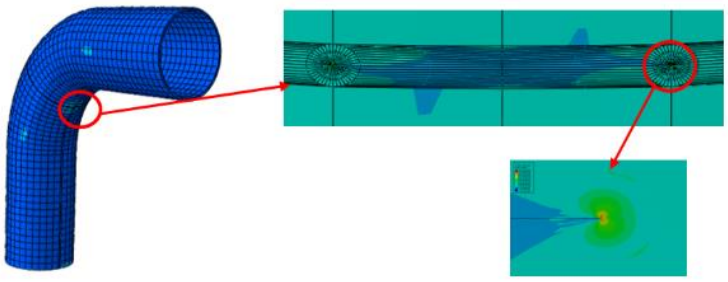

Fig. 12. An example of stress distribution along the crack tip

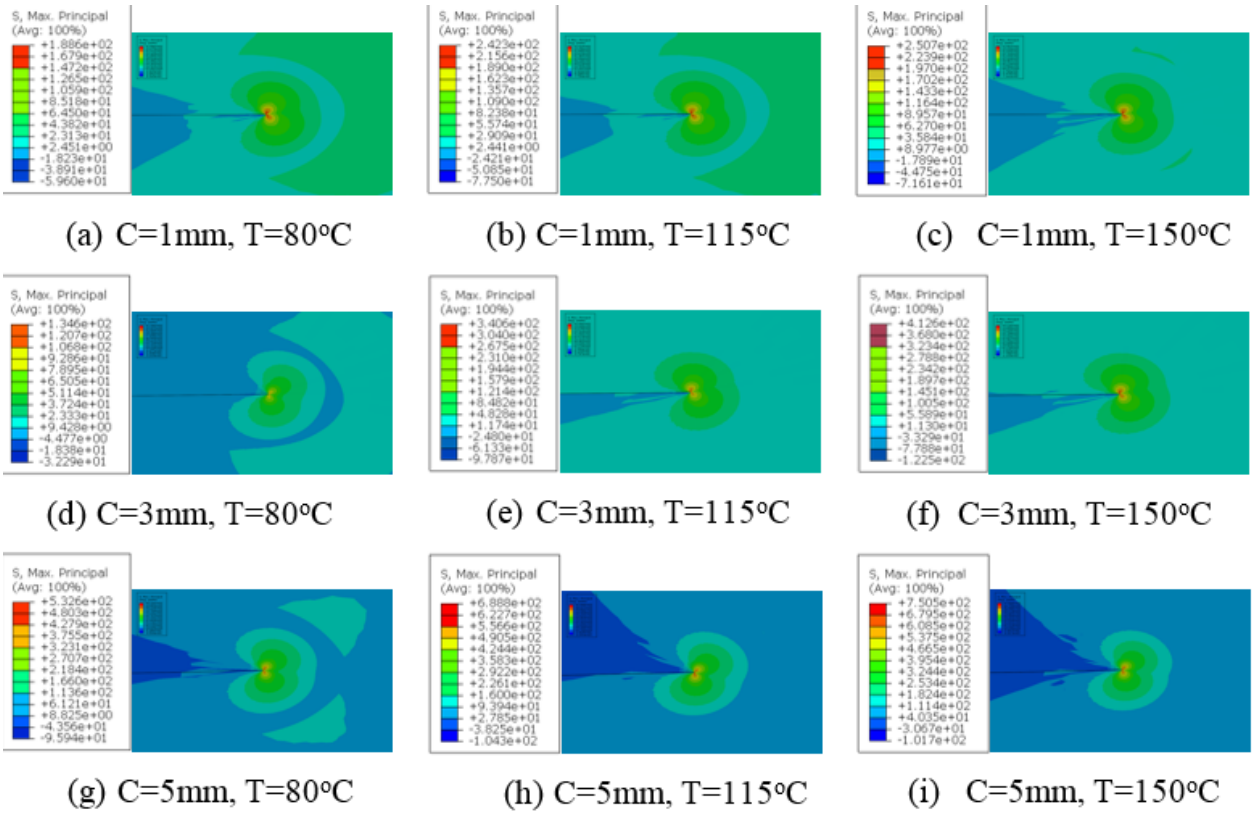

Fig. 13. Contours of stress distribution in front of the crack tip for all variations

The surface crack size of 5 mm has the highest stress intensity factor due to having the greatest crack depth. This is in accordance with the theoretical basis of stress intensity factor as shown in Eq. (3). At a fluid temperature of 150°C has the highest stress intensity factor due to the thermal stress on the pipe is getting bigger by increasing temperature. This is accordance with thermal stress formula i.e.

$$s=\alpha.E.\Delta T \quad (3)$$

where*s* is thermal stress, α is the coefficient of expansion long, E is the modulus of elasticity, and ΔT is the temperature difference [19]. The strength of the geothermal pipe decreased by increasing the thermal stress. This due to the thermal stress is directly proportional to the stress intensity factor. This is according to the theoretical basis of the stress intensity factor formula in Eq. (3). From Figure 5-10, it can be seen that the pipe installation with 5mm crack size and fluid temperature in pipes 115°C and 150°C has stress intensity factor value that exceeds the fracture toughness value of the material. This condition will lead the crack to propagate along the pipe.

4. Conclusions

The present study shows that the stress intensity factor is influenced by fluid temperature and surface crack size in the geothermal pipe installation. The stress intensity factor increased with increasing the fluid temperature in pipe and surface crack size. Furthermore, the pipe installation with 5mm crack size and fluid temperature in pipes 115°C and 150°C has stress intensity factor value that exceeds the fracture toughness value of the material. This condition will lead the crack to propagate along the pipe.

Acknowledgement

This research was funded by a grant from Non Tax Revenues of Brawijaya University (DIPA-042.01.2.400919/2017).

References

[1] Franco, Alessandro, and Maurizio Vaccaro. "On the use of heat pipe principle for the exploitation of medium–low temperature geothermal resources." *Applied Thermal Engineering* 59, no. 1-2 (2013): 189-199.
[2] Dowling, Norman E. (1999). *Mechanical Behavior of Material*. New Jersey: Prentice Hall.
[3] Li, Chun-Qing, Guoyang Fu, and Wei Yang. "Stress intensity factors for inclined external surface cracks in pressurised pipes." *Engineering Fracture Mechanics* 165 (2016): 72-86.
[4] Miranda, José Luis Henríquez, and Luis Alonso Aguirre López. "Piping Design: The Fundamentals." *Short Course on Geothermal Drilling, Resource Development and Power Plant organized by UNU-GTP and LaGeo, in Santa Tecla, El Salvador* (2011).
[5] Tawancy, H. M., Luai M. Al-Hadhrami, and F. K. Al-Yousef. "Analysis of corroded elbow section of carbon steel piping system of an oil–gas separator vessel." *Case Studies in Engineering Failure Analysis* 1, no. 1 (2013): 6-14.
[6] Keera, S. T., N. A. Farid, and K. Z. Mohamed. "Imidazoline Derivatives as Corrosion Inhibitors of Carbon Steel in Crude Oils and Associated Water." *Energy Sources, Part A: Recovery, Utilization, and Environmental Effects* 34, no. 15 (2012): 1371-1383.
[7] Carbon steel handbook. (2007). Palo Alto: Electric Power Research Institute, publication no. 1014670.
[8] Ilman, M. N. "Analysis of internal corrosion in subsea oil pipeline." *Case Studies in Engineering Failure Analysis* 2, no. 1 (2014): 1-8.
[9] Eko Widi Prarnudiohadi, Eko, and Sayogi Sayogi Sudarman. "Duct Pipe Optimation For Geothermal Fluid In Water Dominated Reservoir." In *The 5th Indonesia Geothermal Association Annual Scientific Conference & Exhibitions*. The 5th Indonesia Geothermal Association Annual Scientific Conference & Exhibitions, 2001.
[10] Kusmono and Khasani. "Analysis of a Failed Pipe Elbow in Geothermal Production Facility". *Case Studies in Engineering Failure Analysis* 9, (2017): 71-77.

[11] Firoozabad, Ehsan Salimi, Bub-Gyu Jeon, Hyoung-Suk Choi, and Nam-Sik Kim. "Seismic fragility analysis of seismically isolated nuclear power plants piping system." *Nuclear Engineering and Design* 284 (2015): 264-279.
[12] Firoozabad, Ehsan Salimi, Bub-Gyu Jeon, Hyoung-Suk Choi, and Nam-Sik Kim. "Failure criterion for steel pipe elbows under cyclic loading." *Engineering Failure Analysis* 66 (2016): 515-525.
[13] Pouraria, Hassan, Jung Kwan Seo, and Jeom Kee Paik. "Numerical study of erosion in critical components of subsea pipeline: tees vs bends." *Ships and Offshore Structures* 12, no. 2 (2017): 233-243.
[14] American Society of Mechanical Engineers B 31.3. (2002). Process Piping, ASME Code for Pressure Piping.
[15] Anam, Khairul, and Chih Kuang Lin. "Thermal stress intensity factors of crack in solid oxide fuel cells." In *Applied Mechanics and Materials*, vol. 493, pp. 331-336. Trans Tech Publications, 2014.
[16] Anderson, Ted L. *Fracture mechanics: fundamentals and applications*. CRC press, 2017.
[17] Stephen, Ralph I. (1980). Metal Fatigue in Engineering. Department of Mechanical Engineering, Canada.
[18] Annuar, A.F., Abdul Manan, M.S., Radhwan, H., Khalil, A.N.M., Zakaria, M.Z., and Azmi, H. "Study of Stress Intensity Factors of Primary Crack with Influence of Kerf as Replacement for Subsequent Crack in Multiple Edge Crack Study". *Journal of Advanced Research in Materials Science* 7, (2015): 37-44.
[19] Beer, F.P. and Johnston Jr., E.R. (1981). Mechanics of Materials. McGraw-Hill International Book Company.